This article was downloaded by:
On: *19 January 2011*
Access details: *Access Details: Free Access*
Publisher *Taylor & Francis*
Informa Ltd Registered in England and Wales Registered Number: 1072954 Registered office: Mortimer House, 37-41 Mortimer Street, London W1T 3JH, UK

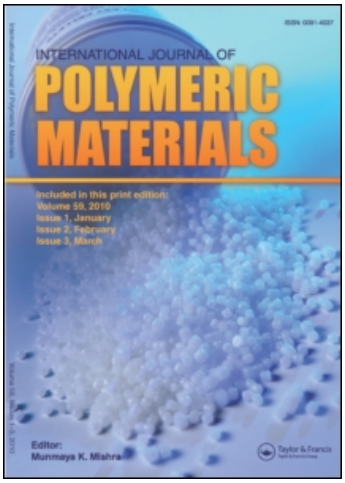

International Journal of Polymeric Materials
Publication details, including instructions for authors and subscription information:
http://www.informaworld.com/smpp/title~content=t713647664

Recent Applications of X-ray Scattering Methods to Fibers and Plastics

R. Zipper[a]
[a] Institute of Physical Chemistry, University of Graz, Graz, Austria

To cite this Article Zipper, R.(2000) 'Recent Applications of X-ray Scattering Methods to Fibers and Plastics', International Journal of Polymeric Materials, 47: 4, 535 — 548
To link to this Article: DOI: 10.1080/00914030008031310
URL: http://dx.doi.org/10.1080/00914030008031310

PLEASE SCROLL DOWN FOR ARTICLE

Full terms and conditions of use: http://www.informaworld.com/terms-and-conditions-of-access.pdf

This article may be used for research, teaching and private study purposes. Any substantial or systematic reproduction, re-distribution, re-selling, loan or sub-licensing, systematic supply or distribution in any form to anyone is expressly forbidden.

The publisher does not give any warranty express or implied or make any representation that the contents will be complete or accurate or up to date. The accuracy of any instructions, formulae and drug doses should be independently verified with primary sources. The publisher shall not be liable for any loss, actions, claims, proceedings, demand or costs or damages whatsoever or howsoever caused arising directly or indirectly in connection with or arising out of the use of this material.

Intern. J. Polymeric Mater., 2000, Vol. 47, pp. 535–548
Reprints available directly from the publisher
Photocopying permitted by license only

© 2000 OPA (Overseas Publishers Association) N.V.
Published by license under
the Gordon and Breach Science
Publishers imprint.
Printed in Malaysia.

Recent Applications of X-ray Scattering Methods to Fibers and Plastics

P. ZIPPER

Institute of Physical Chemistry, University of Graz, Heinrich str. 28, A-8010 Graz, Austria

(Received 15 December 1998)

Downloaded At: 10:34 19 January 2011

X-ray methods are potent and versatile tools for the structural characterization of matter. For our studies on semicrystalline plastics and on parts produced therefrom, we have developed special X-ray scattering techniques which are capable to deliver a wealth of structural information without the necessity to use very expensive equipment or laborious preparations of specimens. Some of the techniques utilizing linear position-sensitive detectors have been applied in the structural characterization of fibers as well. The wide-angle techniques are described and their applications to selected examples, cellulose fibers and cross-sections of moldings from graphite-filled polypropylene, are illustrated.

Keywords: Cellulose; fibers; graphite-filled polypropylene; moldings; wide-angle X-ray scattering (WAXS); site-resolved X-ray studies; morphology; orientation

INTRODUCTION

X-ray scattering methods (small-angle and wide-angle X-ray scattering or diffraction) are very potent and versatile tools for the structural characterization of matter and their applications in studies of fibers and plastics are countless.

Over the last decade, we have performed numerous X-ray investigations on semicrystalline plastics and on parts produced therefrom [1–10] in order to explore the polymer morphology and to elucidate the influence of several factors (molecular characteristics, processing conditions, fillers) especially on the multilayered structures which form during processing. For this purpose, we have developed special techniques, *e.g.*, of site-resolved wide-angle X-ray scattering

(WAXS), which advantageously utilize linear so called position-sensitive detectors (PSD) in order to reduce the measuring time. Some of the techniques have been applied to the structural characterization of fibers as well [11–19].

METHODS

Methods for Investigations of Plastics

Parts which have been produced from semicrystalline thermoplastics such as polypropylene (PP), for example by injection molding, typically possess a multilayered architecture consisting of several layers running approximately parallel to the surface of the parts. These layers may differ in the extent of crystallinity and in the type, size, and orientation of the crystallites and of the supramolecular structures built therefrom. For example, PP may crystallize in various modifications (α, β, γ, mesomorphic PP); usually α-PP is the predominant form, but several forms may co-exist in the same part.

In order to obtain information about the structural characteristics of the various layers in a part, it is necessary to investigate each of the layers separately. In principle, this can be done by mechanical slicing of the parts prior to the X-ray measurements which are then performed on single slices or on packets of several slices. We chose, however, the alternative way of "site-resolved X-ray scattering". In our approach, a cross-section of the part is scanned with a fine X-ray beam that is aligned parallel to the surface of the part (we call this the "parallel transmission geometry"). The advantage of our approach is that we can study the various layers *in situ*, without any mechanical deformations which are likely to occur on mechanical slicing.

Crucial factors in our approach are the collimation of the primary beam and the registration of scattered radiation. The finer the primary beam is collimated the higher is, of course, the feasible spatial resolution of scanning, while the intensity of the beam (and thus also of scattering) is the lower. In order to achieve a high spatial resolution and a high intensity at the same time, we use a Kratky collimation system. This produces a beam having a line-shaped cross-section of about $60\,\mu m \times 2$ mm at the position of the sample. If the line

Downloaded At: 10:34 19 January 2011

is oriented parallel to the surface of the part under investigation, a spatial resolution of about 30 μm along the surface normal becomes feasible. Scanning the cross-section of a 3 mm thick plate thus implies the measurement of X-ray scattering at about 100 equidistant points in the cross-section. This is facilitated by using a computer-controlled step scanning device for a precise positioning of the sample relative to the X-ray beam (minimum step 5 μm). For the registration of scattered radiation we use a position-sensitive detector which allows, with our wide-angle setup, the simultaneous registration of an about 20° broad section of the scattering curve. The entire equipment is installed on a conventional stationary-anode X-ray generator. Cross-sections used for the site-resolved measurements typically are small rectangular blocks of 2 to 10 mm in length, 2 to 3 mm in the direction of X-ray transmission, and about 0.3 to 3 mm in the direction normal to the parts' surface. With such samples, the measuring time for each scattering curve typically is about 400 s. We are hopeful that the intended installation of an additional optical device (Goebel mirror) will bring about a considerable reduction of measuring time.

Downloaded At: 10:34 19 January 2011

The output of a site-resolved WAXS experiment is a 2D intensity diagram, showing scattering curves (intensity *vs.* scattering angle) in dependence on the depth (*i.e.*, the distance of the measuring position from the "reference surface"). Typically the intensities of the reflections in this diagram are not constant but show more or less pronounced variations over the cross-section (*cf.* Fig. 1). A quantitative analysis of the intensity distributions of the reflections finally yields depth profiles of several parameters informing *i.a.* about the crystallite modifications being present and about the type and degree of crystallite orientation (*cf.* Fig. 2). However, before such informations can be deduced from the intensity diagrams it is necessary to separate the contributions of the non-crystalline ("amorphous") phase from those of the crystallites. This step, which is performed in different ways, *e.g.*, by fitting polynomials to the minima in the scattering curves, is usually followed by a modelling of the crystallite scattering curves by means of pseudo-Voigt functions in order to resolve overlapping peaks.

In site-resolved WAXS measurements using the parallel transmission geometry, only those lattice planes can contribute to the measured intensity which are inclined to the surface of the parts by a few degrees. This fact is the basis for the following strategy.

Measurements on cross-sections with the primary beam perpendicular to the flow direction yield basic information about the extent of orientation. Additional details can be obtained from two further measurements, with the primary beam parallel and anti-parallel to the flow direction, respectively (*cf.* Fig. 3).

X-ray experiments were also performed using the classical "symmetrical reflection" and "normal transmission" geometries. Both kinds of experiments yield integrated information. With the symmetrical reflection geometry of a diffractometer, the information refers to lattice planes being exactly parallel to the surface and comprises all those planes between the surface and a depth of about 0.5 mm. The normal transmission experiment, performed with the X-ray beam transmitting the specimen perpendicular to the part's surface, registers the scattering from lattice planes which are inclined to the surface normal by a few degrees and averages over the entire thickness of the part.

The latter experiment was performed with a two-circle goniometer that uses a pinhole-collimated point-shaped primary beam and is also equipped with a linear PSD. Computer-controlled stepwise rotation of the sample around the primary beam results in a 2D intensity diagram showing scattering curves in dependence on the azimuth angle. Such azimuthal intensity distributions can be analyzed to yield information about the preferential orientation of lattice planes relative to the flow direction, in terms of mean square cosines or Hermans' crystalline orientation factor derived therefrom. This analysis usually requires a separation of crystalline and non-crystalline contributions, which is performed for each curve in a similar way as described above.

The two-circle goniometer was also applied to perform site-resolved measurements of the azimuthal intensity distribution on cross-sections of parts, using the parallel transmission geometry. The spatial resolution in these experiments is only about 300 μm, due to the size of the diameter of the beam. Systematic investigations of this kind over entire cross-sections are rather time-consuming and were performed only with few selected samples. The intended installation of a pin-hole camera on a high-power generator with rotating anode and the use of a 2D detector shall reduce the measuring times for such experiments greatly.

Downloaded At: 10:34 19 January 2011

Methods for Investigation of Fibers

Besides the classical measurements of equatorial and meridional scattering by means of a diffractometer, we also performed measurements of azimuthal intensity distributions using the two-circle goniometer with the linear PSD. If the range of scattering angles to be explored exceeded the range accessible with one setting of the PSD, measurements were performed in two subsequent cycles, with the PSD alternately placed at two different scattering angles which were chosen such that the scattering curves obtained from the two measurements overlapped and could be merged into one curve.

The 2D intensity distributions which were obtained in this way (*cf.* Fig. 5) were evaluated either in terms of mean square sines or cosines and orientation factors in order to characterize the degree of fiber orientation, or they were integrated and converted to randomized scattering curves and finally evaluated in terms of crystallinity. For studies of orientation, the separation between non-crystalline and crystalline contributions to the total intensity usually was performed in a similar way as described above, by fitting polynomials to selected minima of each scattering curve (*cf.* Fig. 6).

In the case of cellulose fibers, the azimuthal distributions of the total intensity and of the background, at the scattering angles corresponding to the reflections (101) and ($10\underline{1}$), were first subtracted and the resulting curves were then approximated by pseudo-Voigt and/or Gauss functions ("method A"). For the ($10\underline{1}$) reflection this approximation was essential in order to get rid of disturbing contributions from the (021) reflection (Fig. 8). In an alternative approach ("method B") the azimuthal distributions of total intensity and background were first approximated by pseudo-Voigt and/or Gauss functions (Fig. 7) and the background-correction was performed afterwards, again omitting the contributions of the (021) reflection ("method B").

SAMPLES AND APPARATUS

The following samples were investigated:

- Rectangular plates, injection molded from PP (grade Daplen PT551 from PCD Polymer) filled with up to 40% (w/w) graphite (grades

Downloaded At: 10:34 19 January 2011

AM9060 and SBL2 from Grafitbergbau Kaisersberg; for shortness designated as A and S) [20]. Cross-sections were taken from the plates at distances of 15, 60 and 105 mm from the gate.

- Fibers of regenerated cellulose (from Lenzing AG).

The following apparatus were used:

- Diffractometer Siemens D 500 with Huber texture attachment, Ni filtered Cu radiation, 40 kV, 30 mA.
- Two-circle goniometer Anton Paar with linear detector Braun PSD 50 M, Ni filtered Cu radiation, 50 kV, 45 mA.
- Kratky collimation system (Anton Paar) with 40 μm entrance-slit, home-made sample positioning attachment and vacuum tube, linear detector Braun PSD 50 M, Ni filtered Cu radiation, 50 kV, 45 mA.

Downloaded At: 10:34 19 January 2011

RESULTS AND DISCUSSION

Investigations of PP Parts

The 2D intensity diagrams of a plate molded from unfilled PP (Fig. 1a) show only little variation of the intensities of the main reflections of α-PP with the depth, at all distances from the gate. These diagrams are typical of low-oriented PP. On the contrary, the 2D diagrams of all plates molded from graphite-filled PP show a quite

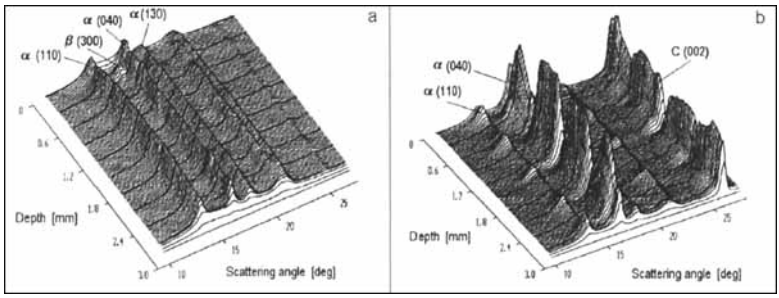

FIGURE 1 2D intensity diagrams, derived from site-resolved WAXS studies in parallel transmission geometry on cross-sections from plates injection molded from (a) unfilled and (b) graphite-filled (10% graphite S) PP. The cross-sections were taken 15 mm from the gate; the direction of transmission was perpendicular to the flow direction. Indices are given for selected reflections of α- and β-PP, and graphite (C).

different behavior (*cf.* Fig. 1b), namely a greatly enhanced intensity of the PP (040) reflection, increasing with the graphite concentration, and considerable variations of the intensities of all PP reflections with the depth. The variations are most pronounced with the (040) reflection. The intensity of the (002) reflection of graphite expectedly increases with the graphite concentration and shows similar variations over the cross-sections as the PP (040) reflection. 2D diagrams referring to different distances from the gate or different graphite grades exhibit only moderate differences.

Quantitative analyses of the 2D diagrams in terms of the orientation parameters A_{110} and C (*cf.* [4, 7]) led to depth profiles like those shown in Figure 2. The parameter C expresses the relative contribution of the (040) reflection to the sum of intensities of the reflections (110), (130) and (040). Its magnitude increases from a level of about 0.4, found for the unfilled PP, up to values > 0.9 for samples of graphite-filled PP. On the other hand, the parameter A_{110}, which usually measures the degree of (fiber) orientation of PP and often reaches its maximum value of 1 in the surface layers of moldings (*e.g.* [6, 7]), decreases in the core region well below its initial level of about 0.5.

Downloaded At: 10:34 19 January 2011

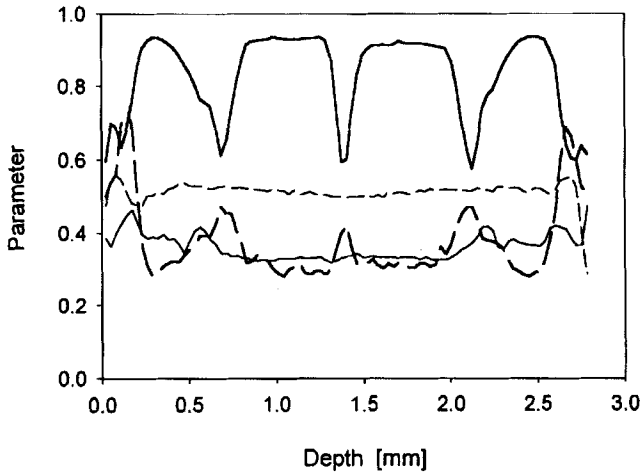

FIGURE 2 Depth profiles of orientation parameters A_{110} (dashed lines) and C (solid lines), derived from the 2D diagrams shown in Figure 1. The thin lines refer to unfilled, the thick ones to graphite-filled PP. Values of $C \approx 1$ indicate a high degree of orientation of α-PP crystallites with the (040) planes parallel to the part's surface.

The behavior of both parameters suggests that in the graphite-filled PP samples the crystallites are highly oriented in a special manner, with the (040) planes parallel to the surface. This conclusion is strongly supported by additional investigations using the two-circle goniometer both in normal and parallel transmission geometry and the diffractometer (data not shown). Those measurements also confirmed the assumption that the graphite particles are oriented preferentially with their (002) planes parallel to the surface. Systematic variations in the inclination may be deduced from Figure 3.

In order to illustrate the role of graphite for the extent of orientation of PP, the values of the parameter C and of the intensity of the graphite reflection were averaged over each cross-section and plotted *versus* the graphite concentration (Fig. 4). The figure shows that a strong increase of the mean parameter C already occurs at graphite concentrations of 1% or lower. Graphite concentrations higher than 10% do not cause an essential further enhancement of the mean value of C, but may even result in a slight decrease of the mean value.

Downloaded At: 10:34 19 January 2011

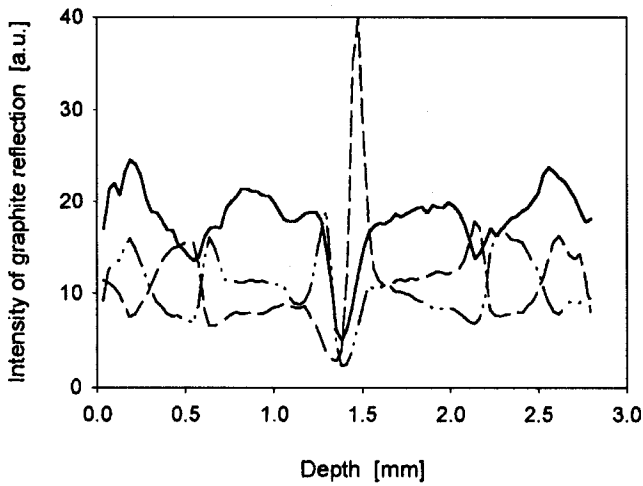

FIGURE 3 Depth profiles of the intensity of graphite (002) reflection, obtained by site-resolved WAXS measurements on cross-sections, using different directions of transmission: perpendicular (solid line), parallel (dashed), and antiparallel (dot-dashed line) to the flow direction. Crossings between the two latter curves indicate changes in the preferential inclination of graphite planes relative to the flow direction.

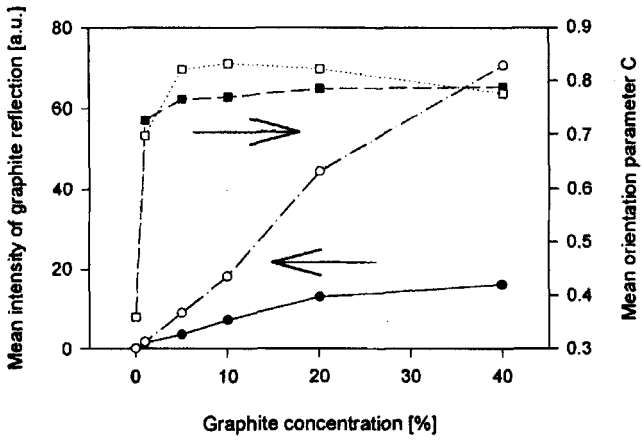

FIGURE 4 The dependence of the mean intensity of graphite reflection (solid and dot-dashed lines) and of the mean orientation parameter C (dashed and dotted lines) on the weight fraction of graphite. Open symbols refer to graphite S, closed ones to graphite A. The mean values were obtained by averaging the depth profiles of parameters (pertaining to 15 mm from gate, perpendicular to flow direction) over the cross-section.

Downloaded At: 10:34 19 January 2011

According to our findings, oriented graphite particles act as nucleators for PP and transfer their mode of orientation to the nascent PP crystallites, causing them to grow perpendicular to the graphite (002) planes. This leads to the observed parallelism of the PP (040) planes with the graphite (002) planes and with the surface of the plates [21].

Investigations of Cellulose Fibers

A bundle of parallelized cellulose fibers was investigated in the two-circle goniometer in normal transmission geometry, using counting times of 1200 s for each scattering curve. The fiber bundle was rotated around the primary beam by 180°, in steps of 2.5° and 5°, respectively. The resulting 2D azimuthal distribution of total intensity is shown in Figure 5. In order to arrive at the azimuthal intensity distributions of the reflections (101) and (10$\underline{1}$) of cellulose II, we followed the procedures outlined in the section Methods. The determination of the background due to non-crystalline cellulose is illustrated in Figure 6, for the equatorial and one meridional scattering curve. The intensities of the total scattering curves and of the background curves at the

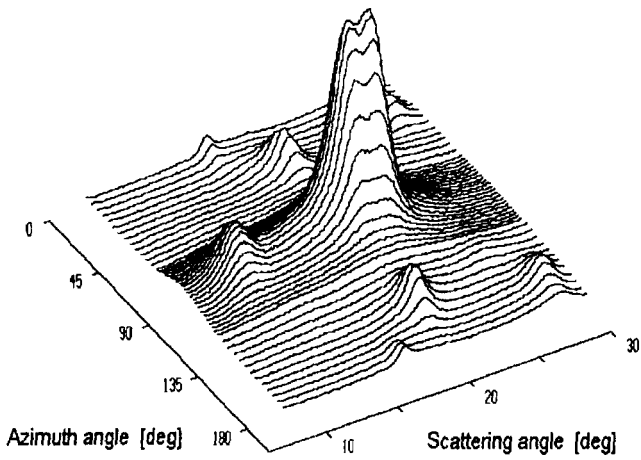

FIGURE 5 2D azimuthal intensity distribution of cellulose fibers, derived from measurements by means of a two-circle goniometer equipped with linear PSD. The plot shows the scattering curves which were obtained at different azimuth angles Φ.

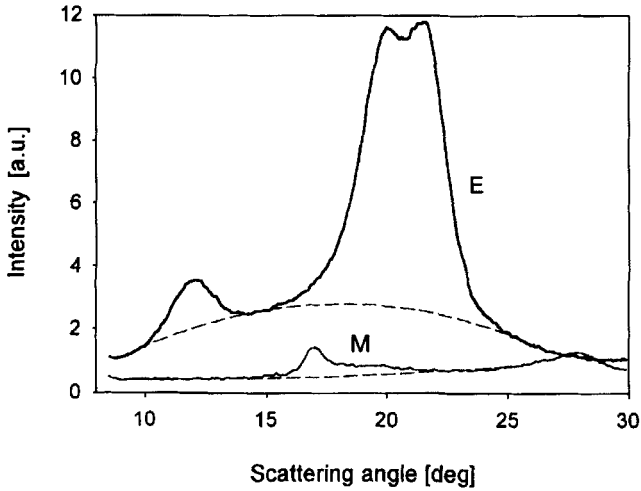

FIGURE 6 Separation of the background (dashed lines) due to non-crystalline phase and incoherent scattering from the equatorial (E) and meridional (M) total scattering curves of cellulose fibers.

scattering angles of 12.29° and 20.02° were used to construct profiles of azimuthal distributions of the reflections (101) and (10$\underline{1}$) and of the corresponding background. These are shown in Figure 7 as raw data

Downloaded At: 10:34 19 January 2011

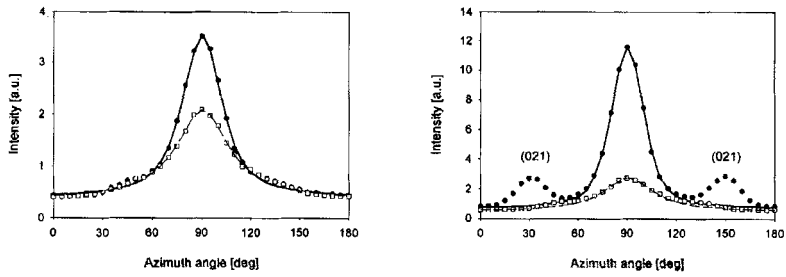

FIGURE 7 Azimuthal distributions of total intensity (circles) and background (squares) for the (101) reflection (left) and the (10$\underline{1}$) and (021) reflections (right) of cellulose fibers. The solid and dashed lines show the approximations by pseudo-Voigt functions. The (021) reflections were modelled by Gaussians (curves not shown).

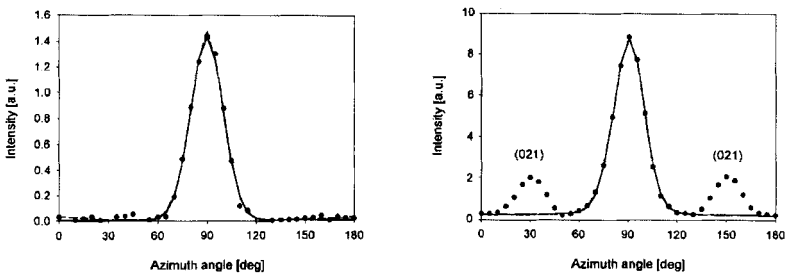

FIGURE 8 Azimuthal intensity distributions of the (101) reflection (left) and the (10$\underline{1}$) reflection (right) of cellulose fibers. The circles show the raw distributions obtained according to method A, the solid lines are the corresponding approximations by pseudo-Voigt functions. Almost identical distributions are obtained by means of method B (dashed lines, hardly visible).

(the curves represented by circles and squares). The profile of the (10$\underline{1}$) reflection also contains contributions from the reflection (021).

Subtraction of the raw data in Figure 7 yielded the background-corrected azimuthal distributions of the reflections (101) and (10$\underline{1}$) shown as raw data (circles) in Figure 8. In order to eliminate the disturbing contributions from the (021) reflection, the raw data in Figure 8 were approximated, using a pseudo-Voigt function for the (10$\underline{1}$) peak and Gaussians for the (021) peaks. Only the data of the (10$\underline{1}$) peak were then used in the further evaluation. For compatibility reasons, the raw data of the (101) reflection were also approximated by a pseudo-Voigt function. The approximated distributions resulting

Downloaded At: 10:34 19 January 2011

from this evaluation procedure (designated as "method A") are shown in Figure 8 as solid lines.

In the alternative evaluation procedure called "method B", the raw data in Figure 7 were first approximated to yield the curves drawn as solid and dashed lines and then subtracted. The resulting intensity distributions of the (101) and (10$\underline{1}$) reflections are presented in Figure 8 as dashed lines. They are nearly identical with the profiles obtained by method A.

Based on the approximated background-corrected profiles (Fig. 8) the mean square cosines $\langle\cos^2\Phi_{101}\rangle$ and $\langle\cos^2\Phi_{10\underline{1}}\rangle$ were calculated. These are identical with the mean square sines $\langle\sin^2\alpha_0\rangle$ and $\langle\sin^2\alpha_3\rangle$ used by Hermans [22] and were evaluated in terms of the mean square sine $\langle\sin^2\beta\rangle$ and the crystalline orientation function f_c accordingly. The results are summarized in Table I.

Downloaded At: 10:34 19 January 2011

As follows from the tabulated values, both evaluation schemes yielded nearly identical results for this sample showing a high degree of orientation. Investigations were also performed on additional 13 samples of different perfection of orientation and evaluated in the same way as the sample presented here. The comparison of the results obtained for those samples from the two evaluation schemes (data not presented) showed a good agreement in most of the cases. Considering the values for f_c, 6 samples gave standard deviations $< 1\%$, for further 4 samples the standard deviation was $< 2\%$. A pronounced discrepancy (standard deviation 14%) was, however, encountered with one sample of low degree of orientation.

In our studies the background due to the non-crystalline phase was explicitly taken into account. By applying the background correction we followed suggestions made by Kratky [23]. Calculation of the orientation factor from the total intensities, omitting the background correction but taking into account the correction for the contributions from the (021) reflection, would have led to considerably lower

TABLE I Mean square sines and crystalline orientation function of the cellulose sample

Evaluation	$\langle sin^2\alpha_0\rangle$	$\langle sin^2\alpha_3\rangle$	$\langle sin^2\beta\rangle$	f_c
method A	0.034	0.066	0.100	0.850
method B	0.033	0.064	0.097	0.855

values for f_c. For the sample presented here, a value of about 0.57 resulted in this way. On the other hand, an evaluation of the azimuthal distribution of the background in terms of an orientation function led for this sample to a value of about 0.37.

CONCLUSION

The examples presented above convincingly demonstrate the capabilities of our X-ray approaches for studies on plastics and fibers.

References

[1] Fleischmann, E., Zipper, P., Jánosi, A., Geymayer, W., Koppelmann, J. and Schurz, J. (1989). Investigations of the layered structure of injection-molded polypropylene discs and of its behavior in tensile tests. *Polym. Eng. Sci.*, **29**, 835–843.

[2] Zipper, P., Jánosi, A. and Wrentschur, E. (1990). Röntgenweitwinkeluntersuchungen an Spritzgußteilen aus isotaktischem Polypropylen. *Österr. Kunststoff Z.*, **21**, 54–59.

[3] Zipper, P., Jánosi, A., Wrentschur, E. and Abuja, P. M. (1991). Small- and wide-angle X-ray scattering investigations of injection-moulded polypropylene. *J. Appl. Cryst.*, **24**, 702–708.

[4] Zipper, P., Jánosi, A., Wrentschur, E., Knabl, C. and Abuja, P. M. (1993). Ortsaufgelöste Röntgenbeugung an Kunststoff-Formteilen. II. Darstellung von Formteilquerschnitten durch Weitwinkelmessungen mittels eines ortsempfindlichen Detektors. *Österr. Kunststoff Z.*, **24**, 162–165.

[5] Zipper, P., Gobec, G. and Kukla, C. (1995). Schichtstrukturen in Zweikomponentenspritzgußteilen. *Österr. Kunststoff Z.*, **26**, 14–15.

[6] Zipper, P., Abuja, P. M., Jánosi, A., Wrentschur, E., Geymayer, W., Ingolic, E. and Friesenbichler, W. (1995). Comparative wide-angle X-ray and microscopical studies on the layered structure in injection molded polypropylene disks. *Intern. Polym. Process.*, **10**, 341–350.

[7] Zipper, P., Jánosi, A., Geymayer, W., Ingolic, E. and Fleischmann, E. (1996). Comparative X-ray scattering, microscopical and mechanical studies on rectangular plates injection molded from different types of isotactic polypropylene. *Polym. Eng. Sci.*, **36**, 467–482.

[8] Zipper, P., Geymayer, W. and Fleischmann, E., X-ray and microscopical investigations of injection molded polypropylene. *SPE/ANTEC 1996 Conference Proceedings (Indianapolis)*, **II**, 2278–2282.

[9] Zipper, P., Eigl, F. and Geymayer, W., Site-resolved X-ray studies on bicomponent injection molded polypropylene plates. *SPE/ANTEC 1997 Conference Proceedings (Toronto)*, **II**, 1534–1538.

[10] Zipper, P., Jánosi, A., Wrentschur, E., Geymayer, W., Ingolic, E., Friesenbichler, W. and Eigl, F. (1997). Wide-angle X-ray, densitometric, and microscopical studies on injection molded polypropylene disks. *Intern. Polym. Process.*, **12**, 192–199.

[11] Gregor-Svetec, D., Malej-Kveder, S., Jánosi, A. and Zipper, P., WAXS structural analysis of polypropylene fibers with higher elasticity moduli. *Proc. 28th International Symposium on Novelties in Textiles*, pp. 311–315, Ljubljana, 1994.

Downloaded At: 10:34 19 January 2011

[12] Sfiligoj Smole, M., Zipper, P. and Jeler, S., Structural changes of PET fibres in supercritical fluids. *Proc. 29th Symposium on Novelties in Textiles*, pp. 311–316, Ljubljana, 1995.
[13] Gregor-Svetec, D., Malej-Kveder, S., Zipper, P. and Jánosi, A. (1995). WAXS structural analysis of polypropylene fibers spun from two different polymer grades. *Chem. Biochem. Eng. Q.*, **9**, 141–143.
[14] Gregor-Svetec, D., Malej-Kveder, S., Zipper, P. and Jánosi, A. (1996). Crystalline structure of polypropylene fibers by wide-angle X-ray scattering analysis. *Acta Chim. Slovenica*, **43**, 21–29.
[15] Gregor-Svetec, D., Malej-Kveder, S., Zipper, P. and Jánosi, A., Structure and properties of polypropylene fibers spun from two different polymer grades. *Proc. 30th International Symposium on Novelties in Textiles*, pp. 87–95, Ljubljana, 1996.
[16] Sfiligoj Smole, M., Zipper, P. and Jeler, S., X-ray diffraction studies of PET fibres. *Proc. 1st International Conference Development, Testing and Application of Materials*, pp. 241–248, Croatian Society for Materials and Tribology, Zagreb, 1996.
[17] Sfiligoj Smole, M., Zipper, P. and Jeler, S., Supercritical fluids and fibre structure. *Proc. 78th World Conf. of the Textile Institute: Textiles and the Information Society*, **III**, pp. 431–440, The Textile Institute, Manchester, 1997.
[18] Gregor-Svetec, D., Malej-Kveder, S., Zipper, P. and Jánosi, A. (1997). Tensile properties and structure of polypropylene fibers spun from a blend of different polymer grades. *Colloid Polym. Sci.*, **275**, 617–626.
[19] Sfiligoj, M. S. and Zipper, P. (1998). WAXS analysis of structural changes of poly(ethylene terephthalate) fibers induced by supercritical-fluid dyeing. *Colloid Polym. Sci.*, **276**, 144–151.
[20] Schnetzinger, K., *Graphitmodifizierte Thermoplaste. Diplomarbeit*, Montanuniversität Leoben, 1997.
[21] Zipper, P. and Schnetzinger, K. (1997). Röntgenstrukturuntersuchungen an Spritzgußplatten aus ungefülltem und grafitgefülltem Polypropylen. 2. Österreichische Polymertage, Rohrmoos, Tagungsband, pp. 15–16.
[22] Hermans, J. J., Hermans, P. H., Vermass, D. and Weidinger, A. (1946). *Rec. Trav. Chim. Pays. Bas.*, **65**, 427–447.
[23] Kratky, O., *Die Physik der Hochpolymeren* (Stuart, H. A., Ed.), **3**, 288–314. Springer, Berlin, 1955.

Downloaded At: 10:34 19 January 2011